Stress-dependent surface reactions and implications for a stress measurement technique

H. H. Yu[a] and Z. Suo[b]
Mechanical and Aerospace Engineering Department and Materials Institute, Princeton University, Princeton, New Jersey 08544

(Received 3 August 1999; accepted for publication 19 October 1999)

In contact with an environment, a solid may gain or lose mass due to, for example, deposition or etching. As the reaction proceeds, the surface of the solid moves, either extending or receding. If the solid is under stress, the elastic energy adds to the driving force of the reaction, and may cause the surface to roughen. This phenomenon has recently led to a novel experimental technique to determine the stress state in a solid by using an atomic force microscope to scan the surface profiles before and after etching. Stress is also known to change the mobility of a reaction. By this mechanism, the stress may either roughen or stabilize a flat surface. This article describes a linear perturbation analysis of a three-dimensional solid surface evolving under stress, using a general kinetic law. It is found that when the reaction is near equilibrium, the stress effect on driving force dominates; when the reaction is far from equilibrium, the stress effect on mobility dominates. Under these two conditions, the surface profile spectra have different patterns and length scales. The implications for the stress measurement technique are discussed. It is suggested that the same experimental procedure be used to measure surface energy and activation strains. © *2000 American Institute of Physics.* [S0021-8979(00)04303-6]

I. INTRODUCTION

A solid may lose mass to, or gain mass from, its environment by a surface process. Examples include vapor deposition, chemical etching, and phase transition. Many kinetic processes may determine the velocity of the interface motion. If a phase transition generates a large amount of heat, such as during freezing, heat conduction in the phases may limit the interface velocity. If the two phases have different compositions, such as during solution precipitation, mass diffusion in the phases may limit the interface velocity. If a transition involves a large volume change, such as when a crystalline particle grows in an amorphous matrix, viscous flow of the matrix may limit the interface velocity. In addition to the long-range transport, atoms must leave one phase, react on the interface, and join the other phase. This article analyzes the situations where the long-range transport and deformation are absent or rapid, so that the interface reaction limits its velocity.

As a nominally flat solid surface moves, it either remains flat or becomes wavy. A solid surface can become wavy due to long-range transport, such as surface diffusion in a strained epitaxial film and heat conduction near a solidification front, which will not be discussed in this paper. Mullins[1] studied the effect of surface energy on the evaporation of a solid. If the solid surface is perturbed into a wavy shape, the surface energy causes the solid to evaporate faster at crests than at troughs, so that the wave amplitude decays over time, and the surface flattens. Srolovitz[2] considered the effect of stress. For a perfectly flat surface, a stress applied parallel to the surface induces a uniform stress state in the solid. For a wavy surface, however, the stress field is nonuniform: the magnitude of the stress is larger at troughs than at crests. Consequently, the solid evaporates faster at the troughs than at the crests, so that the wave amplitude grows over time, and the surface roughens. When both surface energy and stress act together, the ratio of the surface energy to the elastic energy defines a length scale: short waves decay, but long waves grow.

These theoretical studies have recently led to a novel experimental technique to measure stress with high spatial resolution. Using an atomic force microscope, Kim *et al.*[3] scanned the surface profiles of a stressed solid before and after etching. They showed that the difference between the two profiles can be used to identify the stress state. The technique was demonstrated with an aluminum alloy.

The analytical studies of Mullins and Srolovitz, as well as the interpretation of the etching experiment, are all based on an idealized kinetic law. Let F be the driving force (i.e., the free energy reduction associated with the solid gaining per unit volume). For a solid under a state of stress and with a curved surface, the driving force is[4]

$$F = g - w - K\gamma. \tag{1}$$

Here g is the free energy difference between atoms in the two bulk phases (i.e., the environment and the unstressed solid), w the elastic energy per unit volume, γ the surface energy per unit area, and K the sum of the principal curvatures ($K>0$ for a solid sphere). The solid gains mass when $F>0$, and loses mass when $F<0$. In the analyses of Mullins and Srolovitz, the flat, unstressed solid is taken to be in equilibrium with the environment, namely, $g=0$. The analyses

[a]Present address: Division of Engineering and Applied Science, Harvard University, Cambridge, MA 02138.
[b]Author to whom correspondence should be addressed; electronic mail: suo@princeton.edu

highlighted the effects of surface and elastic energy. In practice, however, the contribution due to the chemical energy, g, can be much larger than that due to either elastic or surface energy. Nonetheless g by itself does not affect surface stability.

Let R be the reaction rate, namely, the volume of solid gained ($R>0$) or lost ($R<0$) per unit surface area per unit time. These authors assumed that the reaction rate varies linearly with the driving force, namely,

$$R=MF. \tag{2}$$

The proportionality constant M is known as the mobility of the surface. When the reaction process is thermally activated, the mobility may follow the Arrhenius relation

$$M=M_0\exp(-Q/kT), \tag{3}$$

where k is Boltzmann's constant, and T the temperature. The activation energy Q and the preexponential factor M_0 are parameters to fit experimental data. These authors assumed that the mobility M is independent of the applied stress. This kinetic law can be inadequate for two reasons as discussed below.

First, the linearity is expected only when the reaction is near equilibrium and the driving force is small, namely, $F\Omega/kT\ll 1$, where Ω is the volume per atom in the unstressed solid. When reaction is far from equilibrium and the total driving force F is large, the reaction rate usually varies with the driving force exponentially.

Second, the mobility itself can depend on stress. The kinetic law [Eq. (2)] dictates that the reaction rate R depend on the stress through the driving force F, which depends on the stress through the elastic energy density. Because the elastic energy density is quadratic in the stress, this law predicts that the reaction rate is the same for a solid under tension and under compression. The prediction contradicts with experimental observations. Aziz *et al.*[5] showed that, during the crystallization of an amorphous silicon, when the crystalline silicon surface is subject to an in-plane stress, the velocity of the phase boundary increases linearly with the stress, higher when the stress is tensile and lower when the stress is compressive. The experimental data have been interpreted as an effect of the stress state on the mobility.

More recently Aziz and co-workers showed that the stress-dependent mobility affects the stability of a moving surface.[6] Assume that, at the high temperature, the stress in the amorphous silicon is relaxed by viscous flow, and the applied load is fully carried by the crystalline silicon. As shown in Fig. 1, for a wavy phase boundary under an applied stress nominally in the plane of the surface, the magnitude of the stress is higher at troughs than at crests. When the solid is under a compressive stress, the crystallization rate is slower at troughs than at crests, so that the amplitude of the wave amplifies. Conversely, when the solid is under a tensile stress, the amplitude of the wave decays. These predictions were confirmed by Aziz and co-workers with experiments and calculations. The surface instability caused by stress-dependent mobility is different from that caused by elastic energy, where both tension and compression cause instability.

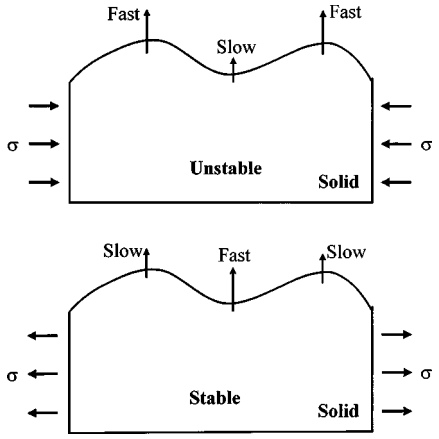

FIG. 1. A solid gains mass. Assume that the reaction rate decreases under compression, and increases under tension. The compression destabilizes a flat surface, and the tension stabilizes a flat surface.

Analogous considerations apply to processes like etching, when the solid loses mass to the environment. The conclusion, however, is opposite to the case when the solid gains mass from the environment, assuming that the reaction rate still increases linearly with the stress. As shown in Fig. 2, when the solid is under a compressive stress, the etching rate is slower at troughs than at crests, so that the crests will catch up with the troughs, and the wave amplitude decays. Conversely, when the solid is under a tensile stress, the wave amplitude grows.

From these considerations, it is quite clear that the evolution of a surface during reaction depends on how the reaction rate varies with the stress. This dependence has significant implications for the stress measurement technique proposed by Kim and co-workers. Under what conditions is the instability predicted by the simplified kinetic law valid? When it is not valid, what information can be extracted from the etching experiment? This article analyzes surface perturbation on the basis of a general kinetic law, and discusses the implications for the stress measurement technique.

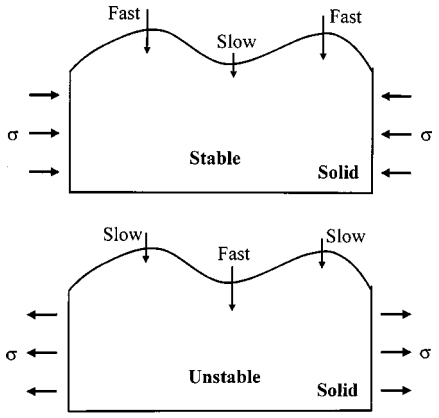

FIG. 2. A solid loses mass. Still assume that the reaction rate decreases under compression, and increases under tension. The compression stabilizes a flat surface, and the tension destabilizes a flat surface.

II. KINETIC LAWS

A surface reaction can be anisotropic in several ways. The reaction rate can be different on different crystal planes, as can the surface energy and elastic constants. A surface reaction can also be inhomogeneous. For example, an optical fiber exposed to water or an acid may roughen or develop etch pits even under no stress.[7] Any structural nonuniformity in the surface, such as defects and impurities, can lead to the observation. To highlight the effect of stress state, in this article the solid is taken to be isotropic and homogeneous with respect to its reaction kinetics, surface energy, and elastic constants. Consequently, the theory should be used with caution in interpreting experiments.

When the driving force is large (i.e., $F\Omega/kT \gg 1$), the reaction rate is no longer linear in the driving force. Often used nonlinear laws include

$$R \propto \sinh\left(\frac{F\Omega}{2kT}\right), \tag{4a}$$

$$R \propto \exp\left(\frac{F\Omega}{kT}\right) - 1, \tag{4b}$$

$$R \propto 1 - \exp\left(\frac{F\Omega}{kT}\right). \tag{4c}$$

These laws are derived from simplistic transition state models, and may not fit perfectly with any real material. Little experimental information is available to favor one form to another.

Next consider the stress effect on mobility. For amorphous-to-crystalline transformation in silicon, the transformation rate is affected by the stress applied in the plane of the phase boundary. The transformation rate increases under a tension, and decreases under a compression.[5] The observation is interpreted as the effect of the stress state on the activation energy, and the experimental data are fit to the following expression:

$$R \propto \exp\left(\frac{-Q + \sigma_{ij}\varepsilon^*_{ij}\Omega}{kT}\right), \tag{5}$$

where the activation strains ε^*_{ij} are parameters to fit experiment data, and Q is the activation energy when the solid is unstressed. Aziz and co-workers[5] retained the first order stress effect on the activation energy (i.e., ε^*_{ij} are taken to be independent of stress). A similar law was used to analyze the shape change of a notch root in a glass, where the second order stress effect on the activation energy was also invoked.[8,9] Because the second order effect on activation energy is likely to be small in the stress range of interest here, we will only consider the first order stress effect. For an isotropic solid, or the (001) surface of a solid of cubic symmetry, the two in-plane activation strain components are equal, $\varepsilon^*_{11} = \varepsilon^*_{22}$. The component normal to the surface, ε^*_{33}, usually differs from the in-plane components. Because in the phenomena of interest here the stress normal to the surface vanishes, ε^*_{33} is irrelevant. Symmetry also dictates that all the shear components of the activation strain tensor should vanish. For the amorphous-to-crystalline transition on the (001) silicon surface, the measured activation strains are $\varepsilon^*_{11} = \varepsilon^*_{22} = 0.14$ and $\varepsilon^*_{33} = -0.56$.[5]

Combining Eqs. (4) and (5), we adopt the kinetic law of the form

$$R = \exp\left(\frac{-Q + \sigma_{ij}\varepsilon^*_{ij}\Omega}{kT}\right) U\left(\frac{F\Omega}{kT}\right). \tag{6}$$

The function U may take the form of one of those in Eq. (4), or any other suitable forms. A representative order of magnitude of the activation strain is $\varepsilon^*_{11} = 0.1$, so that $|\sigma\varepsilon^*_{11}| \gg \sigma^2/E$ for the practical stress range. Consequently, to extract the activation strains from the experimentally measured reaction rates at various stress levels, one may neglect the second order stress effect in the driving force.[5]

In the next section, we derive the surface evolution equation. Rather than committing to a specific form of the kinetic law, we assume that the reaction rate R is a function of the driving force F and the stress tensor σ_{ij}, namely,

$$R = R(F, \sigma_{ij}). \tag{7}$$

The function is taken to have well defined derivatives. The reaction should proceed in the direction of the driving force. Consequently, $R = 0$ when $F = 0$, $R < 0$ when $F < 0$, and $R > 0$ when $F > 0$. It is also assumed that the reaction rate increases with the driving force, namely, $\partial R/\partial F > 0$. The function is otherwise arbitrary. The reaction rate may also depend explicitly on g, or more generally on the composition of the environment. In this article we assume that the mass transport in the environment is so fast that the composition of the environment is uniform during reaction.

We have assumed that the mobility is independent of the curvature. In principle, one may expect that the activation energy depends on the curvature. Analogous to Eq. (5), the leading order curvature effect may be written as

$$R \propto \exp\left(\frac{-Q + K_{ij}\gamma^*_{ij}\Omega}{kT}\right). \tag{8}$$

Here K_{ij} is the curvature tensor, and γ^*_{ij} may be termed as the activation surface energy. One may even speculate on the consequences of the curvature-dependent mobility, and the experiments to detect them. At this point, however, no experimental information is available to us regarding any of these. We will not include the curvature-dependent mobility in the following presentation, although it can be done readily.

III. LINEAR PERTURBATION ANALYSIS

Figure 3 illustrates the problem to be analyzed. A solid gains or loses mass by reacting with an environment. The solid surface is nominally flat and the solid is subject to an in-plane stress state. Denote the principal stresses by σ_1 and σ_2, and the principal axes by x_1 and x_2. At time $t = 0$, the solid occupies the half space $x_3 < 0$, and the environment occupies the half space $x_3 > 0$. At time $t > 0$, the surface height is designated as $H(x_1, x_2; t)$. Decompose the height into the average height $H_0(t)$ and the roughness $h(x_1, x_2; t)$:

$$H(x_1, x_2; t) = H_0(t) + h(x_1, x_2; t). \tag{9}$$

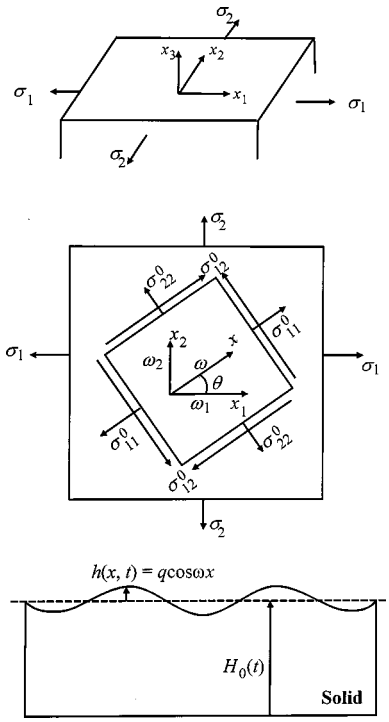

FIG. 3. Geometrical conventions used in the calculations.

In what follows, for a given kinetic law of form of Eq. (7), we will solve for the time evolution of the average height and of the roughness.

When the surface is perfectly flat, the stress state is uniform in the solid, and so is the reaction rate. Consequently, as the solid surface moves, it remains flat and at time t its height is $H_0(t)$. This uniform height can be readily calculated. We look for a solution of surface motion independent of x_1 and x_2. The elastic energy density is

$$w_0=\frac{\sigma_1^2+\sigma_2^2-2\nu\sigma_1\sigma_2}{2E}, \tag{10}$$

where E is Young's modulus and ν Poisson's ratio. When the surface is flat, the curvature K vanishes, and only the chemical energy and the elastic energy contribute to the driving force. Consequently, the driving force of Eq. (1) specializes to $F_0=g-w_0$. At time t, the height of the surface is

$$H_0(t)=tR, \tag{11}$$

where the reaction rate R is evaluated at the uniform driving force F_0 and the uniform stress state σ_1 and σ_2. By recording the average height as a function of the time for surface under various stress states, one can experimentally determine the kinetic law. When $g\gg w_0$, which is often the case, the change in the average height is mainly driven by the chemical free energy.

We next study the time evolution of the surface roughness $h(x_1,x_2;t)$. The roughness is a linear superposition of the Fourier components of wavevectors (lying in the x_1-x_2 plane) of all magnitudes and directions. When the wave amplitude is small, to the first order in the wave amplitude, the stress and the curvature changes due to one Fourier component are independent of those due to another. The time evolution of one Fourier components is independent of another. Consequently, only one representative Fourier component need be analyzed. Figure 3 illustrates a wavevector of magnitude ω pointing in the direction x, which is at an angle θ from the x_1 axis. The two components of the wavevector are $\omega_1=\omega\cos\theta$ and $\omega_2=\omega\sin\theta$. For the time being assume that the roughness has one single Fourier component, which is a cos-wave in the x direction:

$$h=q(\omega,t)\cos\omega x. \tag{12}$$

A linear perturbation analysis will be performed, where the wave amplitude is small compared to the wavelength, namely, $\omega q\ll 1$. Results are retained up to the leading term in the wave amplitude q.

A projection of the velocity $\partial H/\partial t$ to the direction normal to the surface gives the relation $R=\partial H/\partial t[1+(\partial H/\partial x)^2]^{-1/2}$. To the leading order in q, the reaction rate is

$$R=\frac{dH_0}{dt}+\frac{\partial h}{\partial t}. \tag{13}$$

The curvature is defined as $K=-\partial^2 h/\partial x^2[1+(\partial h/\partial x)^2]^{-3/2}$ and, to the leading order in q, is $K=\omega^2 h$.

Figure 3 also illustrates the stress components in the rotated axes, σ_{11}^0, σ_{22}^0, and σ_{12}^0, which relate to the principal stresses as

$$\begin{aligned}\sigma_{11}^0&=\sigma_1\cos^2\theta+\sigma_2\sin^2\theta,\\ \sigma_{22}^0&=\sigma_2\cos^2\theta+\sigma_1\sin^2\theta,\\ \sigma_{12}^0&=-(\sigma_1-\sigma_2)\sin\theta\cos\theta.\end{aligned} \tag{14}$$

When the surface is wavy, the stress state in the solid is nonuniform. The stresses σ_{11}^0, σ_{22}^0, and σ_{12}^0 now serve as boundary conditions.

Denote the stresses in the wavy surface by σ_{11}, σ_{22}, and σ_{12}. To the leading order in the wave amplitude, the stresses in the wavy surface relate to the stresses in the flat surface as

$$\sigma_{ij}=\sigma_{ij}^0+\beta_{ij}h, \tag{15}$$

where β_{ij} must be determined by solving the elasticity boundary value problems of a half space bounded by a wavy surface. When the solid is subject to σ_{12}^0 alone, the surface perturbation $h=q\cos\omega x$ causes a state of antiplane shear deformation. When the solid is subject to σ_{11}^0 alone, because of the constraint of the bulk of the solid, the surface perturbation causes an additional plane strain field. When the solid is subject to σ_{22}^0 alone, the solid with the wavy surface still has the uniform stress σ_{22}^0 throughout the body. The elasticity boundary value problems were solved by Asaro and Tiller, giving[10]

$$\beta_{12}=-\omega\sigma_{12}^0,\ \beta_{11}=-2\omega\sigma_{11}^0,\ \beta_{22}=-2\nu\omega\sigma_{11}^0. \tag{16}$$

Combining Eqs. (15) and (16), one notes that the stresses in the wavy surface linearly depend on the nominal stresses, as expected. More extensive discussion of the problem and literature review can be found in Refs. 11 and 12.

To the leading order in the wave amplitude, the perturbation changes the elastic energy density to

$$w = w_0 - \frac{2(1+\nu)}{E}[(1-\nu)(\sigma_{11}^0)^2 + (\sigma_{12}^0)^2]\omega h. \quad (17)$$

This result agrees with that obtained by another approach.[3] Assembling the above results, we obtain the driving force to the leading order in q as

$$F = F_0 + \alpha h, \quad (18)$$

where

$$\alpha = \frac{2(1+\nu)}{E}[(1-\nu)(\sigma_{11}^0)^2 + (\sigma_{12}^0)^2]\omega - \gamma\omega^2. \quad (19)$$

The significance of this expression will become clear in the next section.

To the leading order in the wave amplitude, the Taylor expansion of the kinetic law in Eq. (7) gives

$$R(F, \sigma_{ij}) = R(F_0, \sigma_{ij}^0) + \left(\frac{\partial R}{\partial F}\alpha + \frac{\partial R}{\partial \sigma_{ij}}\beta_{ij}\right)h. \quad (20)$$

The partial derivatives are evaluated in the state when the surface is flat, (F_0, σ_{ij}^0). A comparison between Eqs. (13) and (20) gives the average surface height [Eq. (11)], as well as the governing equation for the roughness h:

$$\frac{\partial h}{\partial t} = \left(\frac{\partial R}{\partial F}\alpha + \frac{\partial R}{\partial \sigma_{ij}}\beta_{ij}\right)h. \quad (21)$$

Recall that $h = q(\omega, t)\cos \omega x$. Consequently, Eq. (21) is also an equation governing the wave amplitude q.

Integrating Eq. (21) with respect to the time, we obtain that

$$\frac{1}{t}\ln\frac{q(\omega,t)}{q(\omega,0)} = \frac{\partial R}{\partial F}\alpha + \frac{\partial R}{\partial \sigma_{ij}}\beta_{ij}. \quad (22)$$

This equation is a main result of this article. When the quantity on the right-hand side is positive, the wave amplitude grows with the time. Otherwise the wave amplitude decays with the time. Clearly details of the kinetic law will affect the outcome. The remainder of the article is devoted to an analysis of this result.

IV. SURFACE PROFILE SPECTRA

Kim and co-workers[3] recently described a novel technique to experimentally determine the stress state in a small region on a solid surface. A solid surface was under a state of in-plane stress, but the directions and the magnitudes of the principal stresses were unknown. The stressed surface was exposed to an etchant. The surface profiles before and after etching, $h(x_1, x_2; 0)$ and $h(x_1, x_2; t)$, were scanned by using an atomic force microscope. Each surface profile was then represented by the Fourier transform:

$$h(x_1, x_2; t) = \int q(\omega_1, \omega_2; t)\exp i(\omega_1 x_1 + \omega_2 x_2)\, d\omega_1 d\omega_2. \quad (23)$$

The experimentally determined surface profiles were then converted to the value of $\ln[q(\omega_1, \omega_2; t)/q(\omega_1, \omega_2; 0)]$ as a function of the wave numbers ω_1 and ω_2. By comparing this function with the right-hand side of Eq. (22), these authors could deduce the stress state in the surface.

We now study the effect of the kinetic law on this stress measurement technique. Kim *et al.*[3] assumed the linear kinetic law of Eq. (2), the mobility M being independent of stress. One generalization is to allow the reaction rate to be an arbitrary function of the driving force, $R(F)$, still assuming that the explicit dependence on the stress state is negligible. Thus, Eq. (22) becomes

$$\frac{1}{t}\ln\frac{q(\omega,t)}{q(\omega,0)} = \frac{dR}{dF}\alpha. \quad (24)$$

Observe that on the right-hand side, only α depends on the wave number, and $dR/dF > 0$. Consequently, the function $\alpha(\omega_1, \omega_2)$ is identical to $\ln[q(\omega_1, \omega_2; t)/q(\omega_1, \omega_2; 0)]$ up to a constant positive multiplier independent of the wave number. To identify the stress state, one does not need to know the value of this multiplier (see below). The significance of this generalization is evident: to determine the stress state from the spectrum, one does not need to know the kinetic law, so long as the reaction rate depends on the stress only through the driving force.

Substituting Eq. (14) into Eq. (19), one obtains that

$$\alpha = \frac{2(1+\nu)}{E}[(1-\nu)(\sigma_1\cos^2\theta + \sigma_2\sin^2\theta)^2 + (\sigma_1 - \sigma_2)^2\cos^2\theta\sin^2\theta]\omega - \gamma\omega^2. \quad (25)$$

Figure 4 essentially reproduces a figure given in Kim *et al.*,[3] and is included here to compare with other cases later. The two principal stresses play equivalent roles. Furthermore, when both the principal stresses change signs, the value of α is unchanged. Consequently, we need only consider stress states represented on the $\sigma_1 - \sigma_2$ plane within the sector bounded by $\sigma_1 - \sigma_2 = 0$ and $\sigma_1 + \sigma_2 = 0$. Contour plots of $\alpha(\omega_1, \omega_2)$ are given for five representative stress states A, B, C, D, and E. The system has a length scale defined by

$$l = E\gamma/\sigma_1^2. \quad (26)$$

For representative values, $\gamma = 1$ J/m^2, $E = 10^{11}$ N/m^2 and $\sigma_1 = 10^8$ N/m^2, the characteristic length scale is $l = 10^{-5}$ m. The coordinates of the contour plots, $\omega_1 l$ and $\omega_2 l$, are made dimensionless by using the characteristic length scale. Poisson's ratio is taken to be 0.3 in the plots.

For each contour plot, the contour $\alpha(\omega_1, \omega_2) = 0$ is drawn by a darker curve. Inside the darker curve, $\alpha > 0$, and the corresponding Fourier components grow over time. Outside the darker curve, $\alpha < 0$, and the corresponding Fourier components decay over time. Under an equal-biaxial stress state (A), the contours are concentric circles, and α reaches peak when $\omega l = 1 - \nu^2$, which is a circle on the $\omega_1 - \omega_2$ plane. Under the uniaxial stress state (C), the contour plot has two peaks at $\omega l = 1 - \nu^2$, corresponding to the fastest growing Fourier components; after some time, the solid surface will grow into a shape of periodic trenches normal to the σ_1 direction. Under the pure shear stress state (E), the contour plot has four peaks at $\omega l = 1 + \nu$; after some time the solid surface will grow into a shape of periodic islands.

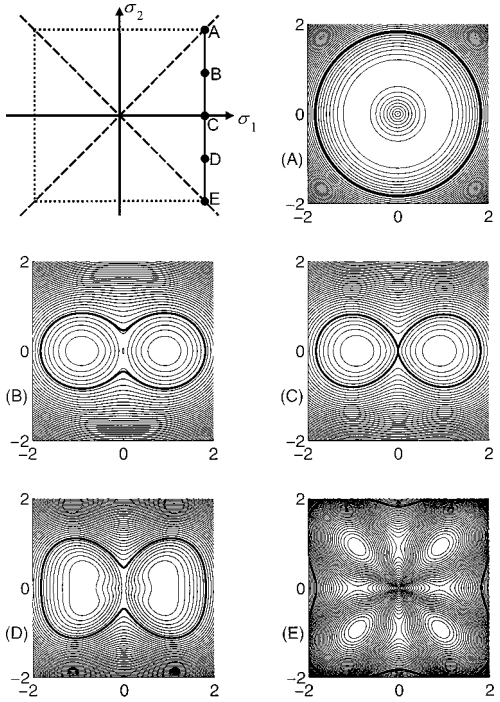

FIG. 4. Surface roughness spectra for reactions near equilibrium (adapted from Ref. 3). On the plane of the principal stresses, five representative stress states A–E are indicated. For each stress state, a contour plot of $\ln[q(\omega_1,\omega_2;t)/q(\omega_1,\omega_2;0)]$ is given. The horizontal axis is $\omega_1 l$, and the vertical axis $\omega_2 l$, where l is a length scale defined in the text. Along the darker contour, $\ln[q(\omega_1,\omega_2;t)/q(\omega_1,\omega_2;0)]=0$, i.e., the wave amplitude does not change with the time. These plots can be used as fingerprints to identify the stress state.

Recall that the experimentally measured data, $\ln[q(\omega_1,\omega_2;t)/q(\omega_1,\omega_2;0)]$, are identical to these contour plots up to a constant positive multiplier. Consequently, these contour plots serve as ''fingerprints'' to identify the stress state. Regardless of the stress state, the contour plots are always symmetric about the two principal stress axes. This symmetry allows the principal axes to be identified from the experimental spectrum. The shape of a contour plot determines the ratio of the two principal stresses, σ_2/σ_1. The size of a contour plot (i.e., the location of the peaks or the $\alpha=0$ contour) determines the characteristic length l. Provided the elastic constants and the surface energy are known, the stress state is determined by such contour plots. The surface energy itself can also be measured this way by subjecting the solid to a known stress state. Note that the absolute values of the contour levels play no role in this technique.

This technique cannot determine the sign of the stress; if the sign of all stress components are changed, the contour plot remains the same. The spatial resolution of this technique is obviously affected by the homogeneity of the surface in response to the etchant, and by the resolution of the atomic force microscope. In addition, at sufficiently large wave numbers, $\omega l \gg 1$, the surface evolution is dominated by the surface energy, and the contours are insensitive to the stress state. Consequently, the length scale l also limits the spatial resolution of this stress measurement technique.

V. EFFECT OF STRESS-DEPENDENT MOBILITY

To study the effect of the stress-dependent mobility, we need to assume a specific kinetic law. An often used kinetic law takes the form

$$R = R_0 \exp\left(\frac{-Q+\sigma_{ij}\varepsilon^*_{ij}\Omega}{kT}\right)\sinh\left(\frac{F\Omega}{2kT}\right). \tag{27}$$

This law was used in the numerical analysis of the surface stability.[6] Equation (22) is specialized to

$$\frac{1}{t}\ln\frac{q(\omega,t)}{q(\omega,0)} = \frac{\Omega R_0}{2kT}\exp\left(\frac{-Q+\sigma^0_{ij}\varepsilon^*_{ij}\Omega}{kT}\right)\cosh\left(\frac{F_0\Omega}{2kT}\right) \times\left[\alpha+2\beta_{ij}\varepsilon^*_{ij}\tanh\left(\frac{F_0\Omega}{2kT}\right)\right]. \tag{28}$$

In the above expression only α and β_{ij} depend on the wave number. Consequently, the quantity in the bracket on the right-hand side of Eq. (28) as a function of the wave number is identical to $\ln[q(\omega_1,\omega_2;t)/q(\omega_1,\omega_2;0)]$ up to a constant positive multiplier independent of the wave number. Now to plot the quantity in the bracket as a function of the wave number, one needs to know the activation strain, and the value of F_0. Usually, $w_0\Omega/kT \ll 1$; for example, to make strain energy comparable to kT, stress should be at the level above 7 GPa at room temperature. Consequently, the magnitude of F_0 is typically dominated by g. One can measure the value of $\varepsilon^*_{11}\tanh(g\Omega/kT)$ by subjecting a surface to a known stress, and perform a spectrum analysis similar to that described above. After the value of $\varepsilon^*_{11}\tanh(g\Omega/kT)$ is determined experimentally, one can construct contour plots for various stress states, and use them as fingerprints to identify unknown stress state.

Note that $\tanh(F_0\Omega/2kT)$ is a number between -1 to 1. We next consider three special cases.

Case 1. The reaction is near equilibrium

In this case, $F_0\Omega/2kT \to 0$, and the bracket in Eq. (28) becomes just α. The result is the same as discussed before. To neglect the activation strain term, one needs to ensure that $|\varepsilon^* g\Omega/kT| \ll |\sigma/E|$.

Case 2. The reaction is far from equilibrium and the solid gains mass

In this case, $F_0\Omega/2kT \to +\infty$ and $\tanh(F_0\Omega/2kT)=+1$. For a representative activation strain $\varepsilon^*_{11}=0.1$, observe that $|\sigma\varepsilon^*_{11}| \gg \sigma^2/E$ for the practical stress range. Consequently, we can neglect the quadratic stress terms in α, and the bracket in Eq. (28) becomes

$$-\gamma\omega^2 - 4(1+\nu)(\sigma_1\cos^2\theta+\sigma_2\sin^2\theta)\varepsilon^*_{11}\omega. \tag{29}$$

When this quantity is negative, the amplitude of the Fourier component decays over time. When this quantity is positive, the amplitude of the Fourier component amplifies. Another length scale is identified:

$$l^* = \gamma/|\sigma_1\varepsilon^*_{11}|. \tag{30}$$

Taking representative values, $\gamma=1$ J/m^2, $\varepsilon^*_{11}=0.1$, and $\sigma_1=10^8$ N/m^2, the characteristic length scale is $l^*=10^{-7}$ m.

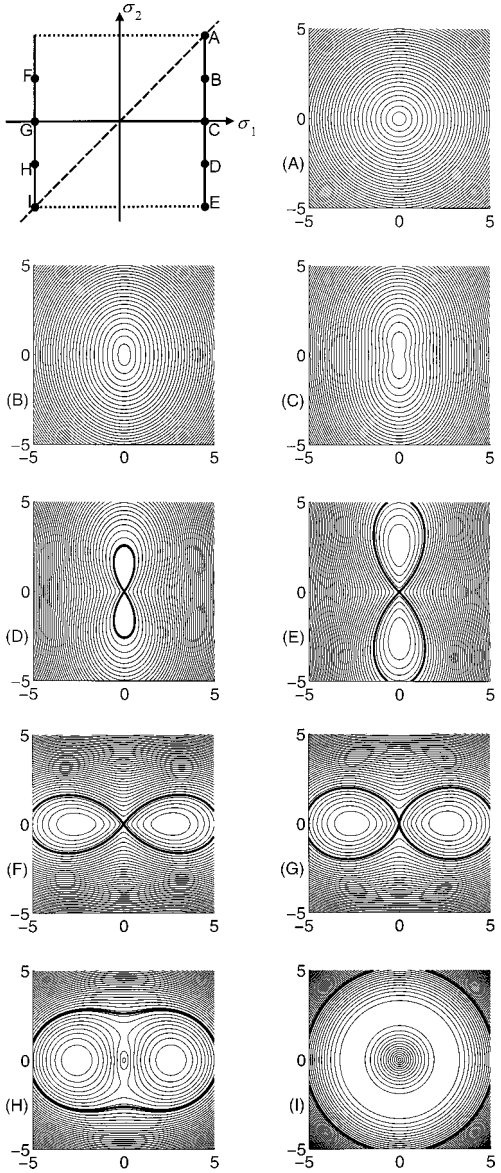

FIG. 5. Surface roughness spectra for reactions far from equilibrium. On the plane of the principal stresses, nine representative stress states A–I are indicated. For each stress state, a contour plot of $\ln[q(\omega_1,\omega_2;t)/q(\omega_1,\omega_2;0)]$ is given. The horizontal axis is $\omega_1 l^*$, and the vertical axis $\omega_2 l^*$, where l^* is a length scale.

This length scale is two orders of magnitude smaller than the length scale l identified above, Eq. (26). Consequently, when the reaction is far from equilibrium, the stress measurement technique can have higher spatial resolutions.

Figure 5 shows the contour plots of Eq. (29), where the coordinates are made dimensionless as $\omega_1 l^*$ and $\omega_2 l^*$. Poisson's ratio is taken to be 0.3 in the plots. The two principal stresses play equivalent roles, so that we restrict the discussion to stress states where $|\sigma_1| \geqslant |\sigma_2|$. Because of the linear dependence on the stress, when both the principal stresses change signs, the contour plots change. Consequently, in addition to the stress states A, B, C, D, and E, four other stress states F, G, H, and I are selected in Fig. 5. We assume $\varepsilon_{11}^* > 0$ in this discussion. When both the principal stresses are tensile (A,B,C), all the Fourier components decay over time. When one or both principal stresses are compressive (D–I), the Fourier components inside the darker contours grow, and the Fourier components outside the darker contours decay. The stress-dependent mobility do not give rise to the four-peak plots under any stress state. Under equal-biaxial compression (I), the contour plot peaks along a circle of radius $\omega l^* = 2(1+\nu)$. Under uniaxial compression (G), the contour plot peaks at two points with $\omega l^* = 2(1+\nu)$.

If one uses the same procedure of Kim *et al.*[3] to determine the stress state, one needs to know the activation strain, in addition to the surface energy. The activation energy can also be determined in similar experiments if one subject to the solid to a known stress state.

Case 3. The reaction is far from equilibrium and the solid loses mass

In this case, $F_0\Omega/2kT \to -\infty$ and $\tanh(F_0\Omega/2kT) = -1$. An etching or a dissolution process of a solid is such an example. The quantity in the bracket in Eq. (28) becomes

$$-\gamma\omega^2 + 4(1+\nu)(\sigma_1 \cos^2\theta + \sigma_2 \sin^2\theta)\varepsilon_{11}^*\omega. \tag{31}$$

Comparing Eqs. (29) and (31), we note that the only difference is a sign. If we also assume that $\varepsilon_{11}^* > 0$, then a tensile stress tends to destabilize the surface, while a compressive stress tends to keep the surface flat. The roughness spectra for various stress states are similar to those in case 2, provided one changes the sign of the stresses.

If one is unsure whether kinetic law [Eq. (27)] adequately describes a given experimental system, one may consider using Eq. (6). Equation (27) then becomes

$$\frac{1}{t}\ln\frac{q(\omega,t)}{q(\omega,0)} = \frac{\Omega R_0 U'}{kT}\exp\left(\frac{-Q+\sigma_{ij}^0\varepsilon_{ij}^*\Omega}{kT}\right) \times\left[\alpha + \frac{\beta_{ij}\varepsilon_{ij}^* U}{U'}\right], \tag{32}$$

where U and the derivative U' are evaluated at $F_0\Omega/kT$, which can be approximated by $g\Omega/kT$. One can experimentally determine the number $\varepsilon_{11}^* U/U'$ by using the procedure of Kim *et al.*[3] by subjecting the solid to a known stress state. After the value of $\varepsilon_{11}^* U/U'$ is determined, one can then measure the unknown stress state for the same material system.

VI. CONCLUDING REMARKS

A stress affects a surface reaction by changing either the driving force (a quadratic effect), or the mobility (a linear effect). Both effects cause the surface roughness to change with time. This article analyzes the time evolution on the basis of a general kinetic law. The roughness change is mainly caused by the quadratic stress effect when the reaction is near equilibrium, and by the linear stress effect when the reaction is far from equilibrium. Under the two conditions, the roughness spectra have different patterns and different length scales. The results can be used to interpret experiments. By measuring surface profiles of a solid under a known stress state, one can extract surface properties such as surface energy and activation energy. Once the surface properties are known, one can then use the roughness spectrum patterns as fingerprints to identify the stress state on the solid

surface with high spatial resolution. The theory assumes an isotropic and homogeneous kinetic law. Substantial experimental observations for various solids and etching compositions need be carried out before stresses can be reliably measured by the technique.

ACKNOWLEDGMENTS

The work is supported by the National Science Foundation (Grant No. CMS-9820713).

[1] W. W. Mullins, J. Appl. Phys. **28**, 333 (1957).
[2] D. J. Srolovitz, Acta Metall. **37**, 621 (1989).
[3] K. S. Kim, J. A. Hurtado, and H. Tan, Phys. Rev. Lett. **83**, 3872 (1999).
[4] C. Herring, in *The Physics of Powder Metallurgy*, edited by W. E. Kingston (McGraw-Hill, New York, 1951), pp. 143–179.
[5] M. J. Aziz, P. C. Sabin, and G. Q. Lu, Phys. Rev. B **44**, 9812 (1991).
[6] W. Barvosa-Carter, M. J. Aziz, L. J. Gray, and T. Kaplan, Phys. Rev. Lett. **81**, 1445 (1998).
[7] D. Inniss, Q. Zhong, and C. R. Kurkjian, J. Am. Ceram. Soc. **76**, 3173 (1993).
[8] W. B. Hillig and R. J. Charles, in *High Strength Materials*, edited by V. F. Zackay (Wiley, New York, 1965), pp. 682–705.
[9] T.-J. Chuang and E. R. Fuller, J. Am. Ceram. Soc. **75**, 540 (1992).
[10] R. J. Asaro and W. A. Tiller, Metall. Trans. **3**, 1789 (1972).
[11] M. A. Grinfeld, Scanning Microsc. **8**, 869 (1994).
[12] M. A. Grinfeld, J. Nonlinear Sci. **3**, 35 (1993).